Received December 19, 2021, accepted December 30, 2021, date of publication January 4, 2022, date of current version January 10, 2022.

Digital Object Identifier 10.1109/ACCESS.2021.3140123

Distribution Feeder Parameter Estimation Without Synchronized Phasor Measurement by Using Radial Basis Function Neural Networks and Multi-Run Optimization Method

NIEN-CHE YANG[1], (Member, IEEE), RUI HUANG[2,3], AND MOU-FA GUO[2,4]

[1]Department of Electrical Engineering, National Taiwan University of Science and Technology, Taipei 10607, Taiwan
[2]Department of Electrical Engineering, Yuan Ze University, Taoyuan 32003, Taiwan
[3]State Grid Quanzhou Electric Power Supply Company, Fujian Electric Company, Quanzhou 362000, China
[4]College of Electrical Engineering and Automation, Fuzhou University, Fuzhou 350116, China

Corresponding author: Nien-Che Yang (ncyang@mail.ntust.edu.tw)

This work was supported in part by the Ministry of Science and Technology (MOST), Taiwan, under Grant MOST 110-2622-8-011-012-SB; and in part by the DELTA-National Taiwan University of Science of Technology (NTUST) Joint Research Center.

ABSTRACT In practice, the performance of distribution feeder parameter estimation is limited by the measurement conditions in distribution networks. An accurate mathematical model that considers limited phasor measurements in distribution networks is necessary to estimate feeder parameters. This paper presents a set of modified parameter estimation models for unbalanced three-phase distribution feeders that only require the measurements of voltage amplitudes and power flows. To simplify the calculation process and improve the estimated results, a method combined with a radial basis function neural network (RBFNN) and multi-run optimization method (MRO), namely RBFNN-MRO, is proposed to calculate the parameters of distribution feeders. The relationship between the feeder parameters and the measurement data from the two terminals of the feeder can be mapped perfectly using the RBFNN. Furthermore, the random errors in the measurement device were eliminated using the proposed RBFNN-MRO algorithm. The RBFNN-MRO algorithm can limit the number of neurons in the hidden layer and substantially reduce the training time for each RBFNN. The feasibility of the proposed method was verified using four IEEE test systems. The proposed RBFNN-MRO and RBFNN methods were compared using the maximum absolute percentage error (MAPE) curves. The results reveal that the proposed RBFNN-MRO method has excellent potential for improving the accuracy of feeder parameter estimation even without synchronized phasor measurement.

INDEX TERMS Parameter estimation method, radial basis function neural network (RBFNN), nonlinear relation, three-phase distribution feeder, maximum absolute percentage error (MAPE).

I. INTRODUCTION

A. BACKGROUND

Owing to the lack of traditional energy sources, the penetration of renewable energy is rapidly increasing in distribution grids. The efficiency and complexity involved in the operation and management of distribution networks have increased with the high penetration of renewable energy generation. To manage distributed energy resources, advanced device control and system analysis methods are imperative. The precise parameters of distribution feeders act as the foundation of power system analysis. In practice, utilities often have an error of 25% to 30% in their transmission system level database parameters when compared to the exact measurement [1]. A significant difference between the actual value and the calculated solution of state estimation or other distribution system analysis is produced by feeder parameters with errors of 20% [2]. Therefore, the parameters of the distribution grids should be determined instantaneously, instead of the feeder parameters obtained

The associate editor coordinating the review of this manuscript and approving it for publication was Mauro Gaggero.

by the supervisory control and data acquisition (SCADA) database.

The three approaches to obtain distribution feeder parameters are as follows:

1) Theoretical calculation method: Empirical equations can be used to calculate the impedance and admittance of distribution feeders, according to the grounding condition, line height, line configuration, and other physical characteristics of distribution feeders. In the theoretical calculation, three-phase power systems were assumed to be balanced. Some uncertainties, such as ambient temperature, non-homogeneous soil conductivity, sag in overhead lines, and geometrical configuration of feeders, may have significant effects on the results obtained by theoretical calculations. The time-varying feeder parameters cannot be reflected in the theoretical calculations [2].
2) Parameter measurement method: Feeder parameters can be measured using specific devices under operation or blackout of distribution feeders.
3) Parameter estimation method: Essentially, the feeder parameter estimation method depends on the measurement data at the two terminals of a feeder. The relationship between feeder parameters and data measured at the two terminals of a feeder can be deduced based on the feeder equivalent model. These measurements can be obtained from phasor measurement units (PMUs), SCADA, fault records, and other measurement devices. In recent years, micro-PMUs (μPMUs) have been gradually adopted to monitor the operation states of distribution networks. The measurement data obtained from the μPMUs can be applied to substantially improve the accuracy of the feeder parameter estimation. A parameter estimation method for single-phase and three-phase distribution feeders based on μPMUs was proposed in [3] and [4]. μPMUs are installed only at a few critical nodes in the distribution networks. Hence, the limited measurement quantities, including voltage amplitude, current amplitude, and power measurements, can be applied to distribution feeder parameter estimation by considering the actual measured conditions in distribution networks.

B. LITERATURE REVIEWS

Transmission feeder parameter estimation technology has been implemented with sufficient measured data and three-phase balanced characteristics [5]–[7]. However, it is difficult to calculate the distribution feeder parameters using parameter estimation methods designed for transmission systems. With advanced programs in distribution management systems (DMSs), distribution feeder parameter estimation becomes essential. Parameter estimations in distribution networks focus on determining parameters for distribution feeders, distribution transformers, switch status, etc. The feeder parameters are mainly evaluated based on linear or nonlinear equations that describe the relationship between feeder parameters and measured quantities. Therefore, a precise feeder equivalent model is necessary to derive the parameter estimation equations. In traditional feeder parameter estimation, the unbalanced characteristics of distribution feeders, and the mutual inductance among conductors are not considered. Furthermore, the lack of measured voltage phasors may lead to inaccurate results for parameter estimation.

In [8], an equivalent model was built based on probability theory. To calculate the feeder parameters, regression analysis and the average value method were used. In distribution grids, impedances were estimated using data from terminal node measurements [9]. For low-voltage and large-scale distribution networks, the mutual coupling among phases is ignored. Similarly, a single-phase mathematical model for parameter estimation, based on trigonometric functions and measurements at two terminals of a feeder, was proposed to eliminate the effect of phasors [10].

Asymmetric phase components and unbalanced phase loads may lead to a three-phase imbalance. The characteristics of the three-phase imbalance should be considered in the distribution feeder parameter estimation. An equation set for medium-voltage distribution feeder parameter estimation was solved using the nonlinear regression method [11]. When the degrees of freedom is smaller than zero, infinite solutions can be found. A set of 12 equations was deduced based on an accurate equivalent model of a three-phase distribution feeder. The problem of solving the ill-conditioned matrix is transformed into a nonlinear optimization problem. The voltage phasors at the two terminals of a feeder were used in [12].

Recently, machine learning has emerged as a dominant research area with diverse applications. Neural networks play an essential role in machine learning. Although most neural networks are based on biological principles, the radial basis function neural network (RBFNN) is based on mathematical principles. The RBFNN is typically used in nonlinear mapping, and it features high accuracy, robustness, and reliability. With a relatively short computation time and high precision, the RBFNN has been applied in fault classification [13] and harmonic power-flow calculation [14] in microgrids.

C. AIM AND CONTRIBUTIONS

In our previous work [15], an RBFNN-based parameter estimation method was proposed for three-phase unbalanced distribution feeders based on bus voltage phasors (magnitudes and phase angles) and complex branch power flows measured from two terminals of the feeder. The RBFNN-based method, quasi-Newton method, and multi-run optimization (MRO) methods were compared. The results showed that the proposed RBFNN-based method performs well throughout the possible range of feeder parameters.

Thus far, no method has been developed for the treatment of distribution feeder parameter estimation without

synchronized phasor measurements. In this regard, the contributions of this study are as follows:

1) A mathematical model that does not require synchronized phasor measurement data is proposed to estimate the parameters of the distribution feeders. The proposed model is based on the principle of constant feeder parameters in a specified short period of time. To increase the degrees of freedom, two sets of measurement data at two time instants are used to calculate the constant feeder parameters.
2) The RBFNN algorithm is adopted to map the nonlinear relationship between the unknown feeder parameters and the power and voltage magnitude measurements. The proposed method not only determines the self-impedance parameters, but also calculates the mutual parameters between phases.
3) Furthermore, random errors in the measurements can be eliminated using the proposed RBFNN-MRO method. The proposed RBFNN-MRO method has a high performance even when the possible range of feeder parameters is wider than ±20% of the initial guess, and the random noise in the power measurement is larger than ±5%.

D. PAPER ORGANIZATION

Herein, Section I briefly introduces the background and objectives of this study. Some related literature has been reviewed. In Section II, the basic and modified models for distribution feeder parameter estimation are presented. The RBFNN-based parameter estimation method is proposed in Section III, followed by the RBFNN-MRO method. The feasibility of the proposed method is verified in Section IV using four IEEE standard test systems, and a conclusion is drawn in Section V.

II. THREE-PHASE DISTRIBUTION FEEDER MODEL FOR PARAMETER ESTIMATION

A reasonable distribution feeder model that considers actual measurement conditions is the foundation for parameter estimation. The distribution feeder model proposed in this study not only considers the imbalance of the electrical parameters but also the mutual impedance parameters. Distribution feeders can be divided into overhead lines and underground cables. Overhead lines are widely used in distribution networks because of their low construction costs and convenient maintenance. Usually, shunt admittance parameters in overhead lines are considerably small and can be neglected in parameter estimation.

A. BASIC MODEL WITH VOLTAGE PHASE ANGLES

An unbalanced three-phase distribution feeder model with measurements between node 'm' and node 'n' expressed in a complex form is shown in Fig. 1.

The primitive impedance matrix of the distribution feeder can be represented by a 3 × 3 symmetric matrix as:

$$\mathbf{Z} = \begin{bmatrix} \bar{z}_{aa} & \bar{z}_{ab} & \bar{z}_{ac} \\ \bar{z}_{ba} & \bar{z}_{bb} & \bar{z}_{bc} \\ \bar{z}_{ca} & \bar{z}_{cb} & \bar{z}_{cc} \end{bmatrix} \tag{1}$$

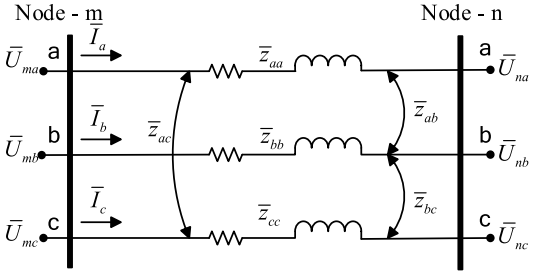

FIGURE 1. Equivalent model of three-phase unbalanced distribution feeder.

The subscripts of the primitive impedance matrix are represented by the phase frame of reference. The diagonal and non-diagonal elements are the self- and mutual impedances of the distribution feeders, respectively. The primitive admittance matrix of the distribution feeders can be obtained by inverting the primitive impedance matrix as:

$$\mathbf{Y} = \begin{bmatrix} \bar{y}_{aa} & \bar{y}_{ab} & \bar{y}_{ac} \\ \bar{y}_{ba} & \bar{y}_{bb} & \bar{y}_{bc} \\ \bar{y}_{ca} & \bar{y}_{cb} & \bar{y}_{cc} \end{bmatrix} = \begin{bmatrix} g_{aa} & g_{ab} & g_{ac} \\ g_{ba} & g_{bb} & g_{bc} \\ g_{ca} & g_{cb} & g_{cc} \end{bmatrix} + j \begin{bmatrix} b_{aa} & b_{ab} & b_{ac} \\ b_{ba} & b_{bb} & b_{bc} \\ b_{ca} & b_{cb} & b_{cc} \end{bmatrix} \tag{2}$$

Therefore, for a structurally symmetric matrix, only 12 parameters $[g_{aa}, g_{ab}, g_{ac}, g_{bb}, g_{bc}, g_{cc}, b_{aa}, b_{ab}, b_{ac}, b_{bb}, b_{bc}, b_{cc}]$ need to be determined. To obtain a unique solution for 12 unknown parameters, 12 independent equations were required for zero degrees of freedom. Therefore, 12 independent equations can be represented by 12 measured electrical quantities, including powers and voltages at both terminals of a feeder. The following equations can deduce the relationship between the power measurements ($P_{kl}, Q_{kl} \forall k \in \{m, n\}$ and $\forall l \in \{a, b, c\}$) and feeder parameters ($g_{lp}, b_{lp} l, p \in \alpha$ and $\alpha = \{a, b, c\}$).

The three-phase branch currents flowing in a distribution feeder can be written as:

$$\begin{bmatrix} \bar{I}_{\mathrm{a}} \\ \bar{I}_{\mathrm{b}} \\ \bar{I}_{\mathrm{c}} \end{bmatrix} = \begin{bmatrix} \bar{y}_{\mathrm{aa}} & \bar{y}_{\mathrm{ab}} & \bar{y}_{\mathrm{ac}} \\ \bar{y}_{\mathrm{ba}} & \bar{y}_{\mathrm{bb}} & \bar{y}_{\mathrm{bc}} \\ \bar{y}_{\mathrm{ca}} & \bar{y}_{\mathrm{cb}} & \bar{y}_{\mathrm{cc}} \end{bmatrix} \begin{bmatrix} \bar{U}_{ma} - \bar{U}_{na} \\ \bar{U}_{mb} - \bar{U}_{nb} \\ \bar{U}_{mc} - \bar{U}_{nc} \end{bmatrix} \tag{3}$$

or

$$\bar{I}_l = \sum_{p=a,b,c} \bar{y}_{lp} (\bar{U}_{mp} - \bar{U}_{np}) \quad \forall l = a, b, c \tag{4}$$

where $\bar{y}_{lp} = g_{lp}+jb_{lp}$, $\bar{U}_{mp} = e_{mp}+jf_{mp}$, and $\bar{U}_{np} = e_{np}+jf_{np}$.

$$\begin{aligned}\bar{I}_l &= \sum_{p=a,b,c} (g_{lp}+jb_{lp})\{(e_{mp}-e_{np})+j(f_{mp}-f_{np})\} \\ &= I_l^r + jI_l^i \end{aligned} \tag{5}$$

Power flow equations can be derived by using branch currents and node voltages.

$$P_{kl} - jQ_{kl} = \left(\bar{U}_{kl}\right)^* \bar{I}_l = e_{kl}I_l^r + f_{kl}I_l^i - j\left(f_{kl}I_l^r - e_{kl}I_l^i\right) \tag{6}$$

Substituting (5) into (6) yields the basic parameter estimation equations as:

$$\begin{aligned}P_{kl} &= e_{kl}\left[\sum_{p=a,b,c}\{g_{lp}\left(e_{mp}-e_{np}\right) - b_{lp}\left(f_{mp}-f_{np}\right)\}\right] \\ &\quad + f_{kl}\left[\sum_{p=a,b,c}\{g_{lp}\left(f_{mp}-f_{np}\right) + b_{lp}\left(e_{mp}-e_{np}\right)\}\right]\end{aligned} \tag{7}$$

$$\begin{aligned}Q_{kl} &= f_{kl}\left[\sum_{p=a,b,c}\{g_{lp}\left(e_{mp}-e_{np}\right) - b_{lp}\left(f_{mp}-f_{np}\right)\}\right] \\ &\quad - e_{kl}\left[\sum_{p=a,b,c}\{g_{lp}\left(f_{mp}-f_{np}\right) + b_{lp}\left(e_{mp}-e_{np}\right)\}\right]\end{aligned} \tag{8}$$

In matrix form, the aforementioned 12 equations can be expressed as

$$\mathbf{PQ} = \mathbf{CD}\cdot\mathbf{gb} \tag{9}$$

where

gb unknown parameter vector;

PQ power measurement vector; and

CD voltage coefficient matrix (10) and (11), as shown at the bottom of the page.

Referring to the different types of power measurements, different nodes, and different phases, the coefficient matrix **CD** can be represented by a partitioned matrix.

$$\mathbf{CD} = \left[\begin{array}{c|c}\mathbf{C_1} & \mathbf{C_2} \\ \hline \mathbf{D_1} & \mathbf{D_2}\end{array}\right] \tag{12}$$

where

$$\mathbf{C_1} = \begin{bmatrix} c_1 & c_3 & c_5 & 0 & 0 & 0 \\ 0 & c_7 & 0 & c_9 & c_{11} & 0 \\ 0 & 0 & c_{13} & 0 & c_{15} & c_{17} \\ c_{19} & c_{21} & c_{23} & 0 & 0 & 0 \\ 0 & c_{25} & 0 & c_{27} & c_{29} & 0 \\ 0 & 0 & c_{31} & 0 & c_{33} & c_{35} \end{bmatrix} \tag{13}$$

$$\mathbf{C_2} = \begin{bmatrix} c_2 & c_4 & c_6 & 0 & 0 & 0 \\ 0 & c_8 & 0 & c_{10} & c_{12} & 0 \\ 0 & 0 & c_{14} & 0 & c_{16} & c_{18} \\ c_{20} & c_{22} & c_{24} & 0 & 0 & 0 \\ 0 & c_{26} & 0 & c_{28} & c_{30} & 0 \\ 0 & 0 & c_{32} & 0 & c_{34} & c_{36} \end{bmatrix} \tag{14}$$

$$\mathbf{D_1} = \begin{bmatrix} d_1 & d_3 & d_5 & 0 & 0 & 0 \\ 0 & d_7 & 0 & d_9 & d_{11} & 0 \\ 0 & 0 & d_{13} & 0 & d_{15} & d_{17} \\ d_{19} & d_{21} & d_{23} & 0 & 0 & 0 \\ 0 & d_{25} & 0 & d_{27} & d_{29} & 0 \\ 0 & 0 & d_{31} & 0 & d_{33} & d_{35} \end{bmatrix} \tag{15}$$

$$\mathbf{D_2} = \begin{bmatrix} d_2 & d_4 & d_6 & 0 & 0 & 0 \\ 0 & d_8 & 0 & d_{10} & d_{12} & 0 \\ 0 & 0 & d_{14} & 0 & d_{16} & d_{18} \\ d_{20} & d_{22} & d_{24} & 0 & 0 & 0 \\ 0 & d_{26} & 0 & d_{28} & d_{30} & 0 \\ 0 & 0 & d_{32} & 0 & d_{34} & d_{36} \end{bmatrix} \tag{16}$$

The coefficient matrix CD is composed of the real and imaginary parts of the voltage phasors, as expressed in (A1)−(A36)for $c_1 - c_{18}$ and $d_1 - d_{18}$. Similarly, $c_{19} - c_{36}$ and $d_{19} - d_{36}$ can be obtained by expanding Equations (7) and (8).

In theory, the feeder parameters can be calculated directly by inverting the coefficient matrix **CD** in (9). Using the quasi-Newton method, accurate solutions can be determined when the voltage phasors and power flows for a feeder are effectively measured [12]. However, the negligible difference between voltage measurements at the two terminals of a feeder may result in ill-conditioning in the coefficient matrix **CD**.

B. PROPOSED MODEL WITHOUT VOLTAGE PHASE ANGLES

Most measured quantities in distribution networks may only include the node voltage amplitude, branch current amplitude, active power, and reactive power. Therefore, the phase angles for node voltages are treated as unknowns. To determine 24 unknowns, 24 independent equations are required.

The modified parameter estimation equations were developed without the measurement data of the voltage phase angles. Based on a reasonable assumption, the variations in the feeder parameters during a short period of time are negligible. From (9), a set of parameters can be calculated from a set of measured powers and voltage phasors at a given measurement. Similarly, two sets of feeder parameters were obtained from two sets of measured quantities for two distinct measurements. The variations in the feeder parameters can be ignored during a short period of time. An identical parameter vector was calculated from the electrical quantities at two distinct measurements. Therefore, the parameter estimation

$$\mathbf{gb} = \begin{bmatrix} g_{aa} & g_{ab} & g_{ac} & g_{bb} & g_{bc} & g_{cc} & b_{aa} & b_{ab} & b_{ac} & b_{bb} & b_{bc} & b_{cc} \end{bmatrix}^t \tag{10}$$

$$\mathbf{PQ} = \begin{bmatrix} P_{ma} & P_{mb} & P_{mc} & P_{na} & P_{nb} & P_{nc} & Q_{ma} & Q_{mb} & Q_{mc} & Q_{na} & Q_{nb} & Q_{nc} \end{bmatrix}^t \tag{11}$$

equation can be modified as

$$\begin{bmatrix} \mathbf{PQ}^1 \\ \mathbf{PQ}^2 \end{bmatrix} = \begin{bmatrix} \mathbf{CD}_1 \\ \mathbf{CD}_2 \end{bmatrix} \cdot \mathbf{gb} \tag{17}$$

where

$\mathbf{CD}_1$, $\mathbf{CD}_2$ coefficient matrices obtained from two distinct measurements; and

$\mathbf{PQ}^1$ and $\mathbf{PQ}^2$ power measurements at two distinct measurements.

(17) can be written in the following alternative form:

$$\mathbf{PQ} = \mathbf{f}\left(\mathbf{gb}, \theta^1, \theta^2\right) \tag{18}$$

where

θ^1, θ^2 the phase angles of the node voltages at two distinct measurements.

$$\theta^1 = \left[\theta^1_{ma}\ \theta^1_{mb}\ \theta^1_{mc}\ \theta^1_{na}\ \theta^1_{nb}\ \theta^1_{nc}\right]^t \tag{19}$$

$$\theta^2 = \left[\theta^2_{ma}\ \theta^2_{mb}\ \theta^2_{mc}\ \theta^2_{na}\ \theta^2_{nb}\ \theta^2_{nc}\right]^t \tag{20}$$

$\mathbf{PQ} = \left[\mathbf{PQ}^1\ \mathbf{PQ}^2\right]^t$ is the measured power at two distinct measurements. In (18), there are 24 power measurements and 24 unknowns. Because of the zero degrees of freedom in (18), a unique solution can be determined.

III. PROPOSED PARAMETER ESTIMATION METHOD

A. RBFNN

Relation fitting is a nonlinear regression problem that can be solved using various neural networks. The RBFNN exhibits excellent performance in terms of approximation ability, classification ability, and learning speed. Therefore, the RBFNN was adopted in this study. The architecture of the RBFNN is shown in Fig. 2.

A pass-through input layer, output layer, and hidden layer were included in the RBFNN. The neurons in the hidden layer map the low-dimensional input vectors to the high-dimensional space using the radial basis function. The coordinate vector of neurons in the hidden layer and the mapping connection of the RBFNN were determined by the training samples. In Fig. 2, an input vector $\mathbf{x} = [x_1, x_2, \ldots, x_n]^t$ is connected to the hidden layer without weight factors. The basis function in the hidden layer is used to transform the input vector $\boldsymbol{x}$ into the output of the hidden layer $\mathbf{h}$ as

$$h_j = e^{-\frac{\|\mathbf{x}-c_j\|^2}{2b_j^2}} \tag{21}$$

where

c_j coordinate vector for the jth neuron in the hidden layer; and

b_j width for the jth neuron in the hidden layer.

Three parameters, including the coordinate vectors $\mathbf{c}$ of the hidden layer, width $\mathbf{b}$ of the Gaussian function, and weights $\mathbf{w}$, are requested in the RBFNN.

In this study, the self-organizing selection center method was used as the learning method for RBFNN [16]. The coordinate vector and width were calculated using the K-means clustering method in the first step. In the second step, the weights between the hidden and output layers are calculated. The specific steps are as follows:

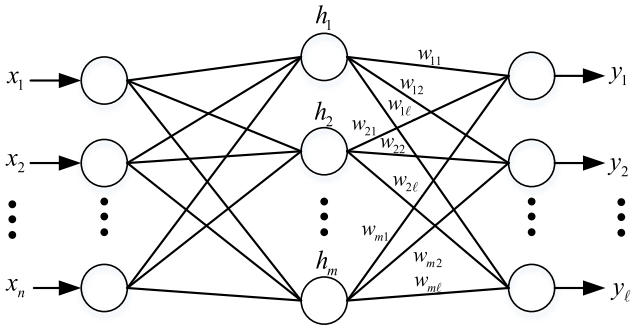

FIGURE 2. Architecture of RBFNN.

***Step* 1**: m training samples were selected as clustering centers. Input vector $\mathbf{x}$ is divided into different cluster sets, according to the Euclidean distance between the input vector $\mathbf{x}$ and the coordinate vector $\mathbf{c}$. Then, the average value of the training samples in each cluster set is regarded as the new cluster center. The coordinate vector is determined when the new cluster center remains unchanged. In contrast, a new cluster is sought continuously.

The width of the Gaussian function is also an essential factor for RBFNN. The wider the width of the Gaussian function, the lower the sensitivity of the RBFNN. Conversely, a smaller width may lead to overfitting of the RBFNN. The width of the Gaussian function is calculated as follows:

$$b_j = \frac{c_{\max}}{\sqrt{2m}} \quad (j = 1, 2, \ldots, m) \tag{22}$$

where

$c_{\max}$ maximum distance between the different coordinate vectors; and

m number of nodes in the hidden layer.

***Step* 2**: The connection weights between the hidden and output layers were then calculated. The RBFNN can approximate the required solution by minimizing the standard error term of (23), by changing the coordinate vectors $\mathbf{c}$ of the hidden layer, the width $\mathbf{b}$ of the Gaussian function, and the weights $\mathbf{w}$.

$$E = \left\|\mathbf{y} - \mathbf{w}^t\mathbf{h}\right\|_2 \tag{23}$$

where

$\|\cdot\|_2$ Euclidean norm.

An exact fit (EF) method [17] was used to determine the relationship between the network output and actual output with zero error. The weights for the RBFNN can be obtained by minimizing the objective function, using the linear least squares method, as follows:

$$\mathbf{w}^t = \mathbf{y}\mathbf{h}^t\left(\mathbf{h}\mathbf{h}^t\right)^{-1} \tag{24}$$

B. PROPOSED RBFNN-BASED METHOD

The RBFNN can approximate arbitrary nonlinear functions with good generalization ability and fast learning

convergence speed. A complex nonlinear relation between feeder parameters and the power measurement in (17) can be mapped using the RBFNN. The actual feeder parameters may vary within a specific range of theoretical parameters provided by the manufacturer. Although the RBFNN has high tolerance, the errors of the power measurement may lead the estimated results to deviate from the actual parameters. Therefore, a methodology is presented to improve the estimated results. This is done by changing the coordinate vector of the RBFNN. A flowchart of the proposed RBFNN-based method is shown in Fig. 3. The specific steps are as follows:

***Step* 1**: The coefficient matrix **CD** is assumed to be constant, and a different power vector **PQ** can be calculated by varying the feeder parameter vector **gb** randomly within a specific range. Different training samples [**gb**; **PQ**] were produced by changing the feeder parameters.

***Step* 2**: The training samples are used to train the RBFNN. The power measurements **PQ** and feeder parameters **gb** are used as the input and output, respectively.

***Step* 3**: Based on the well-trained RBFNN, the feeder parameter vector $\mathbf{gb}'$ can be obtained from the actual power measurement vector $\mathbf{PQ}'$.

***Step* 4**: The estimated parameter vector $\mathbf{gb}'$ is substituted into (17) to calculate a new power measurement vector $\mathbf{PQ}''$. The Euclidean distance (ED) between $\mathbf{PQ}''$ and $\mathbf{PQ}'$ is

$$ED = \left\| \mathbf{PQ}' - \mathbf{PQ}'' \right\|_2 \tag{25}$$

***Step* 5**: If the calculated ED is smaller than the predefined threshold tolerance (10^{-6}), the estimated parameter vector $\mathbf{gb}'$ is regarded as the final solution. Otherwise, the training sample **PQ** with the maximum Euclidean distance (MED) is replaced by a new training sample $\left[\mathbf{gb}'; \mathbf{PQ}''\right]$; the process returns to Step 2 and trains a new RBFNN. In contrast, if the ED between $\mathbf{PQ}'$ and $\mathbf{PQ}''$ is larger than the predefined tolerance and MED, new training data are reproduced to replace the previous data with the MED.

The network structure of the RBFNN was determined using training samples. The coordinate vector, width, and weight can all be calculated using the self-organizing selection center method mentioned in the previous section. Until the mean square error (MSE) between the output of the RBFNN and the actual solution is smaller than the predefined tolerance (10^{-20}), the training of the RBFNN continues.

C. PROPOSED RBFNN-MRO METHOD

The solution vector can be calculated using the RBFNN-based parameter estimation method. The maximum absolute percentage errors (MAPEs) between the estimated solutions obtained by the RBFNN-based method and the actual values may increase with larger measurement errors. Random errors in measurement devices, caused by external interferences, are challenging to predict. However, random errors may significantly affect the accuracy of the estimated solutions. Owing to random errors with a Gaussian normal distribution, the mathematical expectation of the random error is zero [18]. In addition, the deviation of feeder parameters is negligibly

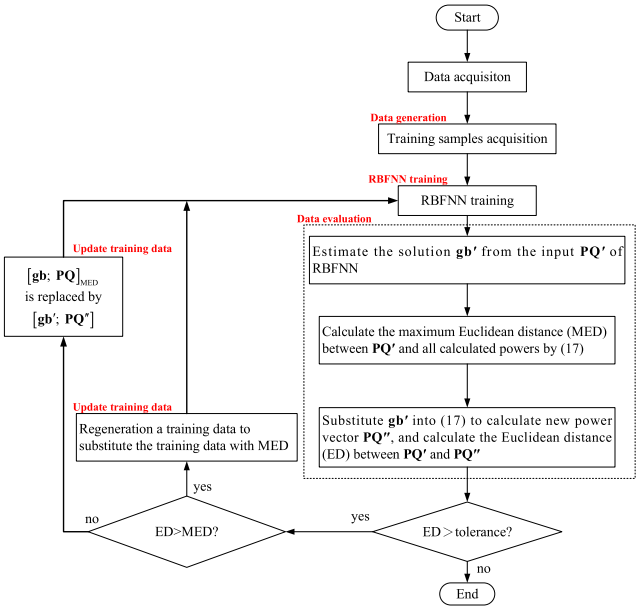

FIGURE 3. Flow chart of the proposed RBFNN-based parameter estimation method.

small during a short period of time. Theoretically, the solution vectors calculated using the measured data at different time instants are identical.

Based on the aforementioned principle, a large number of solutions were estimated by multiple measurements. The random errors in the individual estimated parameters can be canceled by averaging the set of parameter solutions. Therefore, the final solution was approximated to the actual value. To eliminate random errors, the MRO method [12] was used to determine the final solution. The iteration process of the MRO method continues until the difference between the averages of two successive estimated values is less than a predefined threshold. Therefore, the proposed RBFNN-MRO parameter estimation method was used to further reduce the MAPEs. A flowchart of the proposed RBFNN-MRO method is shown in Fig. 4.

The specific steps of the RBFNN-MRO method are as follows:

***Step* 1**: Setting initial values as follows: $iter = 1$, the sum of all estimated admittance parameters $\mathbf{gb}_{total} = 0$, and the average value of all parameters calculated at the last time $\mathbf{gb}_{last} = 0$.

***Step* 2**: Training data are generated by varying the feeder parameters within a specific range. The RBFNN-based parameter estimation method mentioned in Section III.B was used to train the RBFNN.

***Step* 3**: Based on the well-trained RBFNN, a new solution vector $\mathbf{gb}_{new}$ is calculated using two successive test datasets, which are numbered k and k+1.

***Step* 4**: The following calculations are performed: $\mathbf{gb}_{total} = \mathbf{gb}_{total} + \mathbf{gb}_{new}$, average parameter $\mathbf{gb}_{cal} = \mathbf{gb}_{total}/iter$, and maximum tolerance $tol = \max\left(\left|\mathbf{gb}_{cal} - \mathbf{gb}_{last}\right|\right)$. If $tol < 10^{-6}$, the estimate $\mathbf{gb}_{cal}$ is the

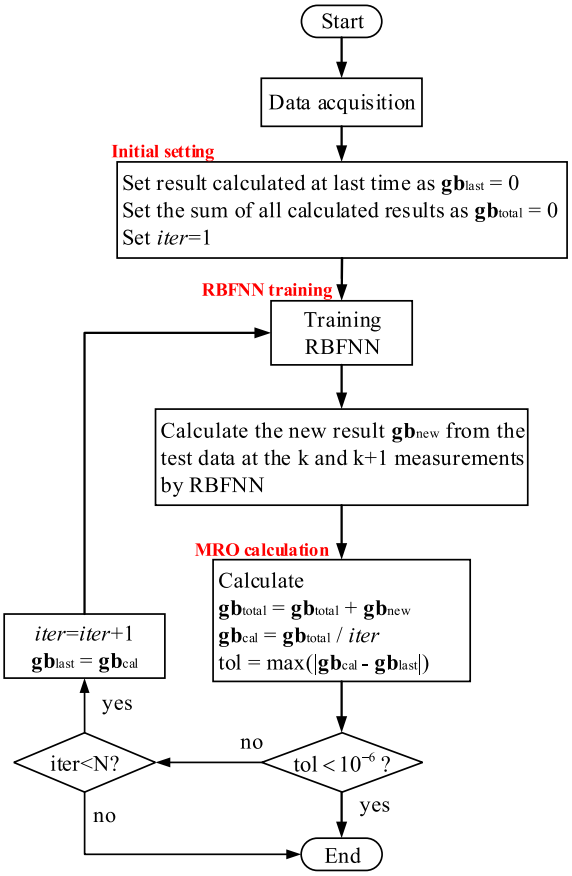

FIGURE 4. Flow chart of the proposed RBFNN-MRO method.

final solution. Otherwise, set $iter = iter + 1$ and $\mathbf{gb}_{last} = \mathbf{gb}_{cal}$, and return to Step 2. If the tolerance threshold is significantly small, the MRO method may require a significant amount of time to obtain the solutions. Furthermore, even if a larger tolerance threshold is selected, the convergence time decreases, and the MAPE increases.

IV. TEST CASES AND RESULTS

In this study, all computer programs were developed using MATLAB 2016a on a Windows 10-based Intel Core i7-2600 personal computer. To test the proposed method, four IEEE test feeders, including the IEEE 13 bus, IEEE 34 bus, IEEE 37 bus, and IEEE 123 bus, were adopted in this study [19]. In the four feeder systems, 191 feeders, including single-phase, two-phase, and three-phase, were adopted for testing.

In the IEEE 13 bus test feeder, the length of the feeders is relatively short, and the power flow at the two terminals is significant. Therefore, the effect of measurement errors on the final solution was minimal. Because of the long feeders in the IEEE 34 bus feeder and the complexity of feeder parameters and measurement data in the IEEE 37 bus feeder and the IEEE 123 bus feeder, the effect of measurement errors on the final solution is obvious.

The deviations of the feeder parameters were almost equal to zero within a specified period. Accuracy is the most important index for the performance of the parameter estimation algorithms. The voltage phasors at each node and power flow of each feeder, both of which were calculated by performing power flow solutions [20] for the four IEEE test feeders, are regarded as actual measured data for testing the proposed methods. Based on the modified parameter estimation model, the proposed methods were verified using four IEEE test feeders. All estimated solutions are expressed in the MAPE form herein. The MAPE was calculated as follows:

$$\text{MAPE} = \max\left(\left|\frac{\mathbf{gb}_{cal} - \mathbf{gb}_{actual}}{\mathbf{gb}_{actual}}\right|\right) \times 100\% \qquad (26)$$

The initial parameters are determined by the historical parameters stored in the DMS or calculated using an empirical formula. In this study, the feeder parameters in [19] were adopted as the initial parameter vectors. The proposed RBFNN-based method and RBFNN-MRO method were verified by the nine case conditions shown in Table 1. The possible range of parameters is considered to be within ±5–20% of the corresponding theoretical values of the feeder section parameters. The power measurement error was considered to be a random noise within the range of ±1–5%.

TABLE 1. Conditions for study case.

Test case	Possible range of parameters	Error of power measurement
Case 1	±5%	±0.5%
Case 2	±10%	±0.5%
Case 3	±20%	±0.5%
Case 4	±5%	±1%
Case 5	±10%	±1%
Case 6	±20%	±1%
Case 7	±5%	±5%
Case 8	±10%	±5%
Case 9	±20%	±5%

The actual solution of the feeder parameter may exist within a possible range of parameters. The different parameters in this range were randomly generated as training data. In this study, the following two-parameter estimation methods were used for comparison:

1. RBFNN-based method;
2. RBFNN-MRO based method.

The RBFNN method is a simple calculation process for the modified parameter estimation model. Based on the proposed model, the parameter estimation can be calculated without requiring the measured voltage phase angles. To limit the training time of the RBFNN, the number of training samples was set to 10,000 for the proposed methods. To test the proposed RBFNN-MRO method, measurement data for a specified period of time is required to calculate the average solution. Therefore, the load model shown in [21] was used as the load demand in the test systems. To assign the load demands to each node at different measured time instants, the sum of the given load data in the IEEE test feeder is set as the annual peak load. The requested load data was calculated using the daily load curves for the individual phases. Then, the measured data at different time instants was

generated. According to the measurement data, the RBFNN-based method is executed repeatedly to determine the average value of the estimated solutions, until the iteration process converges. Two sets of measurement data at two distinct time instants were requested in the modified model for each calculation. A total of 167 sets of measurement data were available. Therefore, the maximum number of iterations for the RBFNN-MRO method was 167. The iteration process is continued until the iteration time reaches 167, or the difference between two successive estimated average solutions is within the predefined tolerance (10^{-6}).

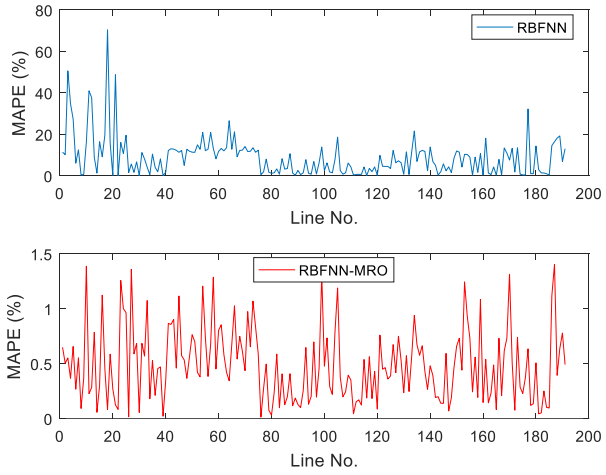

FIGURE 5. MAPEs for case 1.

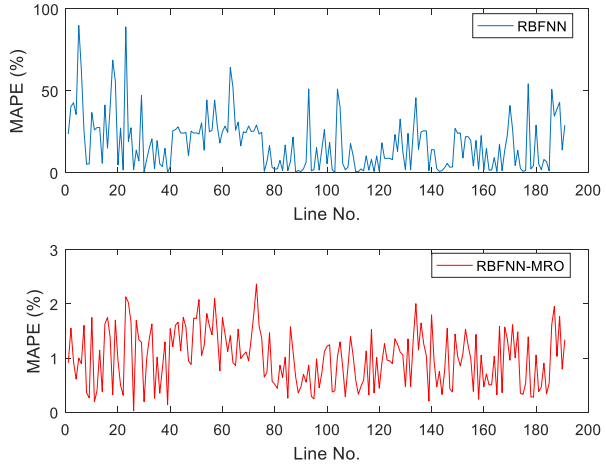

FIGURE 6. MAPEs for case 2.

The MAPEs are shown in Fig. 5−Fig. 13. It can be observed that the MAPEs increase with the extension of the parameter range, when the measurement error remains constant. Similarly, the MAPEs increase with the increase in measurement errors, when the parameter range is kept constant. Both the parameter range and measurement errors have significant effects on the estimated solutions. In other words, numerous unknowns and insufficient training data may result in high errors in the estimated solutions.

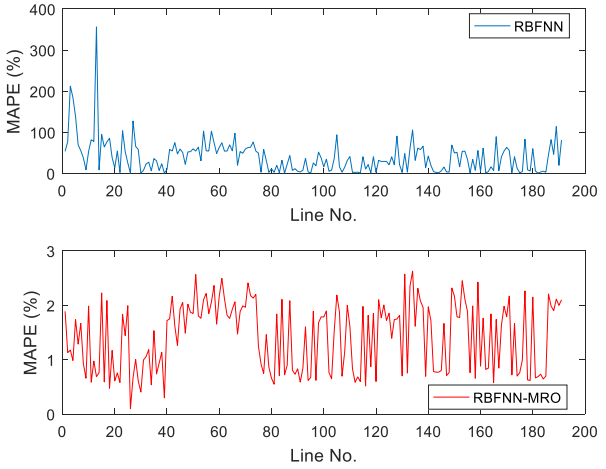

FIGURE 7. MAPEs for case 3.

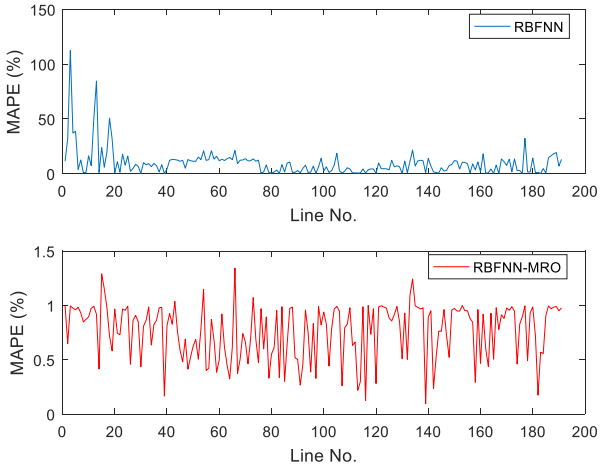

FIGURE 8. MAPEs for case 4.

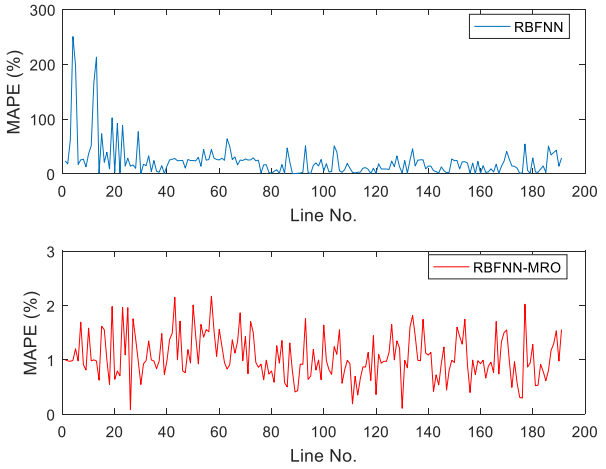

FIGURE 9. MAPEs for case 5.

The accuracy of the RBFNN method can be improved by using sufficient training data. However, a higher hardware configuration is required. A large number of training samples may generate the same number of neurons in the hidden

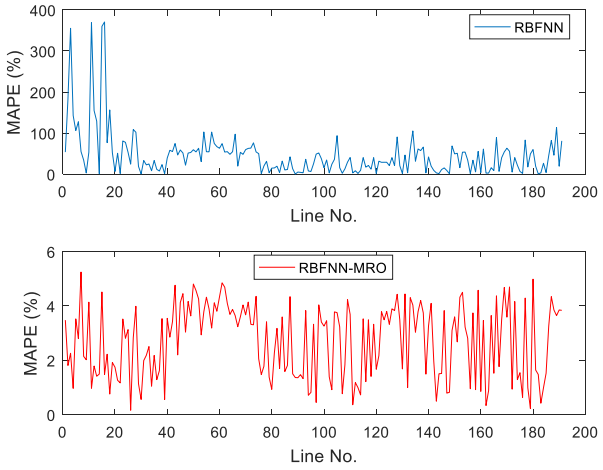

FIGURE 10. MAPEs for case 6.

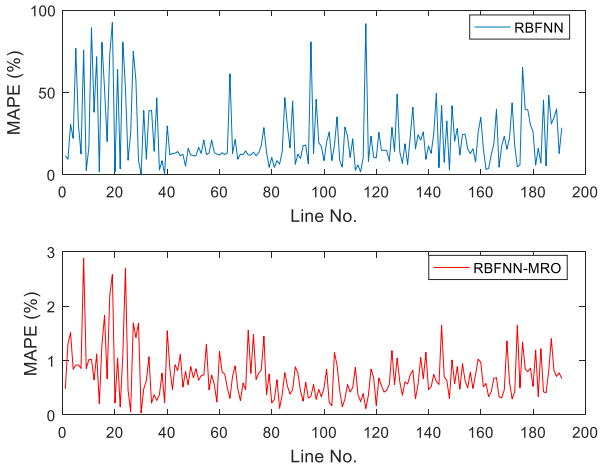

FIGURE 11. MAPEs for case 7.

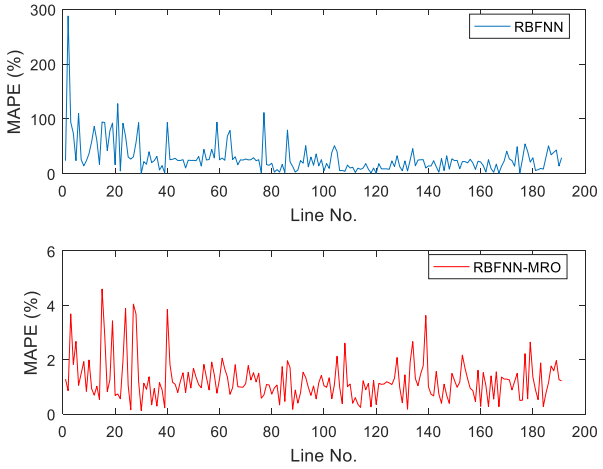

FIGURE 12. MAPEs for case 8.

layer. Correspondingly, the oversized matrix generated in the training process of the RBFNN may significantly exceed the memory limitation of the computer hardware. The MAPEs for the RBFNN-MRO method in the nine test cases are

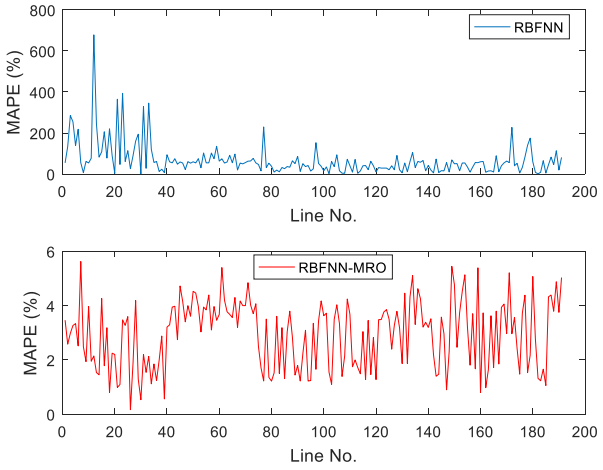

FIGURE 13. MAPEs for case 9.

smaller than 6%, as shown in Table 2. Compared with the RBFNN method, the MAPEs for the RBFNN-MRO method change in a low deviation with a wider parameter range or a significant measurement error. The RBFNN-MRO method can improve the estimated solutions significantly, even if the measurement error increases or the parameter range is extended. Although the computation time of the RBFNN-MRO method is much longer than that of the RBFNN method, the accuracy of the RBFNN method is better than that of the RBFNN-MRO method. Parallel computing can be used in the RBFNN-MRO method to reduce the computation time. The training time for each RBFNN was decreased, and 10,000 training samples were sufficient to obtain accurate solutions.

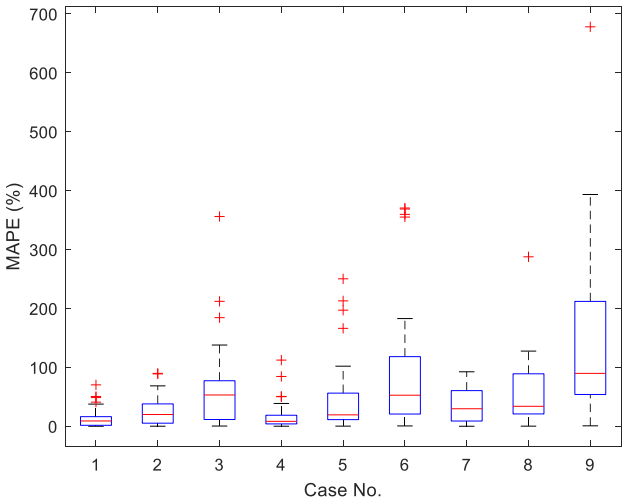

FIGURE 14. Estimation error for the proposed RBFNN method under different cases.

Figs. 14 and 15 show the box-and-whisker diagram for the estimated parameters for nine cases based on the six-number summary:

1. Median (red line): the middle value in the dataset;
2. Minimum (lower end of the dotted line): the lowest data in the dataset excluding outliers;

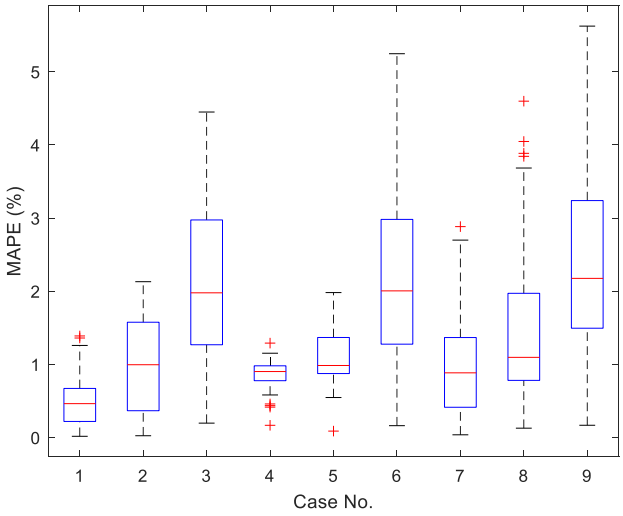

FIGURE 15. Estimation error for the proposed RBFNN-MRO method under different cases.

TABLE 2. RBFNN-based method vs. RBFNN-MRO based method.

Case	RBFNN				RBFNN-MRO			
	Best	Worst	Mean	Std. dev.	Best	Worst	Mean	Std. dev.
Case 1	0.0937	70.4088	8.8958	9.5778	0.0139	1.4051	0.4907	0.3302
Case 2	0.1805	89.8859	17.9734	16.8008	0.0243	2.3657	1.0046	0.5164
Case 3	0.4697	356.1689	40.3032	41.3344	0.0983	2.6260	1.4186	0.6332
Case 4	0.1344	112.4310	9.6481	12.4561	0.0956	1.3435	0.7654	0.2533
Case 5	0.3064	250.4392	22.9756	32.5268	0.0876	2.1702	1.0569	0.4156
Case 6	0.4280	370.6285	46.7358	57.6301	0.1618	5.2456	2.7117	1.3430
Case 7	0.1053	92.5834	22.6759	19.7584	0.0370	2.8826	0.7251	0.4557
Case 8	0.2867	287.7777	28.6899	30.7238	0.1277	4.5969	1.2395	0.7687
Case 9	0.8457	678.2512	67.7048	80.2184	0.1674	5.6228	2.9438	1.2345

3. Maximum (upper end of the dotted line): the highest data in the dataset excluding outliers;
4. First quartile (lower end of the blue box): median of the lower half of the dataset;
5. Third quartile (upper end of the blue box): median of the lower upper part of the dataset;
6. Outliers (red crosses): outliers.

For the RBFNN method, the largest median MAPE was 67.7048% in case 9. For the RBFNN-MRO method, the largest median MAPE was 2.9438% in case 9. The worst-case maximum outlier was 678.2512% for the RBFNN method and 5.6228% for the RBFNN-MRO method.

V. CONCLUSION

In traditional parameter estimation methods, PMUs are used to estimate the magnitude and phase angle of the electrical phasor quantities, using a common time source for synchronization. For cost considerations, PMUs cannot be installed on all nodes in distribution networks. Therefore, mathematical models of distribution feeders, or algorithms with a high tolerance for synchronization should be exploited. In this study, a modified parameter estimation model that does not require voltage phase angles for a three-phase unbalanced distribution feeder is deduced in detail. The nonlinear relationship between the measurement data at both terminals of the feeder and feeder parameters can be mapped expertly by the RBFNN. Therefore, RBFNN-based parameter estimation methods are proposed in this study. As the measurement errors increase, the proposed RBFNN-MRO method exhibits superior performance. The random errors in the power measurement can be eliminated effectively. Meanwhile, the low-performance problem for a large number of training samples in the proposed RBFNN-based method can be solved using the proposed RBFNN-MRO method. The results reveal that the proposed RBFNN-MRO method has good potential for improving the accuracy of feeder parameter estimation, even for ill-measured conditions.

APPENDIX

$$c_1 = e_{ma}(e_{ma} - e_{na}) + f_{ma}(f_{ma} - f_{na}) \quad \text{(A1)}$$
$$c_2 = e_{ma}f_{na} - f_{ma}e_{na} \quad \text{(A2)}$$
$$c_3 = e_{ma}(e_{mb} - e_{nb}) + f_{ma}(f_{mb} - f_{nb}) \quad \text{(A3)}$$
$$c_4 = f_{ma}(e_{mb} - e_{nb}) - e_{ma}(f_{mb} - f_{nb}) \quad \text{(A4)}$$
$$c_5 = e_{ma}(e_{mc} - e_{nc}) + f_{ma}(f_{mc} - f_{nc}) \quad \text{(A5)}$$
$$c_6 = f_{ma}(e_{mc} - e_{nc}) - e_{ma}(f_{mc} - f_{nc}) \quad \text{(A6)}$$
$$d_1 = e_{ma}f_{na} - f_{ma}e_{na} \quad \text{(A7)}$$
$$d_2 = f_{ma}(f_{na} - f_{ma}) - e_{ma}(e_{ma} - e_{na}) \quad \text{(A8)}$$
$$d_3 = f_{ma}(e_{mb} - e_{nb}) - e_{ma}(f_{mb} - f_{nb}) \quad \text{(A9)}$$
$$d_4 = f_{ma}(f_{nb} - f_{mb}) - e_{ma}(e_{mb} - e_{nb}) \quad \text{(A10)}$$
$$d_5 = f_{ma}(e_{mc} - e_{nc}) - e_{ma}(f_{mc} - f_{nc}) \quad \text{(A11)}$$
$$d_6 = f_{ma}(f_{nc} - f_{mc}) - e_{ma}(e_{mc} - e_{nc}) \quad \text{(A12)}$$
$$c_7 = e_{mb}(e_{ma} - e_{na}) + f_{mb}(f_{ma} - f_{na}) \quad \text{(A13)}$$
$$c_8 = f_{mb}(e_{ma} - e_{na}) - e_{mb}(f_{ma} - f_{na}) \quad \text{(A14)}$$
$$c_9 = e_{mb}(e_{mb} - e_{nb}) + f_{mb}(f_{mb} - f_{nb}) \quad \text{(A15)}$$
$$c_{10} = e_{mb}f_{nb} - f_{mb}e_{nb} \quad \text{(A16)}$$
$$c_{11} = e_{mb}(e_{mc} - e_{nc}) + f_{mb}(f_{mc} - f_{nc}) \quad \text{(A17)}$$
$$c_{12} = f_{mb}(e_{mc} - e_{nc}) - e_{mb}(f_{mc} - f_{nc}) \quad \text{(A18)}$$
$$d_7 = f_{mb}(e_{ma} - e_{na}) - e_{mb}(f_{ma} - f_{na}) \quad \text{(A19)}$$
$$d_8 = f_{mb}(f_{na} - f_{ma}) - e_{mb}(e_{ma} - e_{na}) \quad \text{(A20)}$$
$$d_9 = e_{mb}f_{nb} - f_{mb}e_{nb} \quad \text{(A21)}$$
$$d_{10} = f_{mb}(f_{nb} - f_{mb}) - e_{mb}(e_{mb} - e_{nb}) \quad \text{(A22)}$$
$$d_{11} = f_{mb}(e_{mc} - e_{nc}) - e_{mb}(f_{mc} - f_{nc}) \quad \text{(A23)}$$
$$d_{12} = f_{mb}(f_{nc} - f_{mc}) - e_{mb}(e_{mc} - e_{nc}) \quad \text{(A24)}$$
$$c_{13} = e_{mc}(e_{ma} - e_{na}) + f_{mc}(f_{ma} - f_{na}) \quad \text{(A25)}$$
$$c_{14} = f_{mc}(e_{ma} - e_{na}) - e_{mc}(f_{ma} - f_{na}) \quad \text{(A26)}$$
$$c_{15} = e_{mc}(e_{mb} - e_{nb}) + f_{mc}(f_{mb} - f_{nb}) \quad \text{(A27)}$$
$$c_{16} = f_{mc}(e_{mb} - e_{nb}) - e_{mc}(f_{mb} - f_{nb}) \quad \text{(A28)}$$
$$c_{17} = e_{mc}(e_{mc} - e_{nc}) + f_{mc}(f_{mc} - f_{nc}) \quad \text{(A29)}$$
$$c_{18} = e_{mc}f_{nc} - f_{mc}e_{nc} \quad \text{(A30)}$$
$$d_{13} = f_{mc}(e_{ma} - e_{na}) - e_{mc}(f_{ma} - f_{na}) \quad \text{(A31)}$$
$$d_{14} = f_{mc}(f_{na} - f_{ma}) - e_{mc}(e_{ma} - e_{na}) \quad \text{(A32)}$$
$$d_{15} = f_{mc}(e_{mb} - e_{nb}) - e_{mc}(f_{mb} - f_{nb}) \quad \text{(A33)}$$

$$d_{16} = f_{mc}\left(f_{nb} - f_{mb}\right) - e_{mc}\left(e_{mb} - e_{nb}\right) \quad \text{(A34)}$$

$$d_{17} = e_{mc}f_{nc} - f_{mc}e_{nc} \quad \text{(A35)}$$

$$d_{18} = f_{mc}\left(f_{nc} - f_{mc}\right) - e_{mc}\left(e_{mc} - e_{nc}\right) \quad \text{(A36)}$$

REFERENCES

[1] G. L. Kusic and D. L. Garrison, "Measurement of transmission line parameters from SCADA data," in *Proc. IEEE PES Power Syst. Conf. Expo.*, Oct. 2004, pp. 440–445.

[2] J. D. Glover, M. S. Sarma, and T. Overbye, *Power System Analysis & Design*, SI Version. Cengage Learn., 2012.

[3] P. A. Pegoraro, K. Brady, P. Castello, C. Muscas, and A. V. Meier, "Line impedance estimation based on synchrophasor measurements for power distribution systems," *IEEE Trans. Instrum. Meas.*, vol. 68, no. 4, pp. 1002–1013, Apr. 2019.

[4] R. Puddu, K. Brady, C. Muscas, P. A. Pegoraro, and A. Von Meier, "PMU-based technique for the estimation of line parameters in three-phase electric distribution grids," in *Proc. IEEE 9th Int. Workshop Appl. Meas. Power Syst. (AMPS)*, Sep. 2018, pp. 1–5.

[5] E. C. M. Costa and S. Kurokawa, "Estimation of transmission line parameters using multiple methods," *IET Gener., Transmiss. Distrib.*, vol. 9, no. 16, pp. 2617–2624, 2015.

[6] C. S. Indulkar and K. Ramalingam, "Estimation of transmission line parameters from measurements," *Int. J. Elect. Power Energy Syst.*, vol. 30, no. 5, pp. 337–342, Jun. 2008.

[7] D. Shi, D. J. Tylavsky, K. M. Koellner, N. Logic, and D. E. Wheeler, "Transmission line parameter identification using PMU measurements," *Eur. Trans. Elect. Power*, vol. 21, no. 4, pp. 1574–1588, 2011.

[8] D. Jia, W. Sheng, X. Song, and X. Meng, "A system identification method for smart distribution grid," in *Proc. Int. Conf. Power Syst. Technol.*, Oct. 2014, pp. 14–19.

[9] W. Luan, J. Peng, M. Maras, J. Lo, and B. Harapnuk, "Smart meter data analytics for distribution network connectivity verification," *IEEE Trans. Smart Grid*, vol. 6, no. 4, pp. 1964–1971, Jul. 2015.

[10] A. M. Prostejovsky, O. Gehrke, A. M. Kosek, T. Strasser, and H. W. Bindner, "Distribution line parameter estimation under consideration of measurement tolerances," *IEEE Trans. Ind. Informat.*, vol. 12, no. 2, pp. 726–735, Apr. 2016.

[11] B. Vicol, M. Gavrilas, O. Ivanov, B. Neagu, and G. Grigoras, "Synchrophasor measurement method for overhead line parameters estimation in MV distribution networks," in *Proc. 16th Int. Conf. Harmon. Quality Power (ICHQP)*, May 2014, pp. 862–865.

[12] B. Das, "Estimation of parameters of a three-phase distribution feeder," *IEEE Trans. Power Del.*, vol. 26, no. 4, pp. 2267–2276, Oct. 2011.

[13] M. Mirzaei, M. Z. A. A. Kadir, H. Hizam, and E. Moazami, "Comparative analysis of probabilistic neural network, radial basis function, and feed-forward neural network for fault classification in power distribution systems," *Electr. Power Compon. Syst.*, vol. 39, no. 16, pp. 1858–1871, Oct. 2011.

[14] H. R. Baghaee, M. Mirsalim, G. B. Gharehpetian, and H. A. Talebi, "Unbalanced harmonic power sharing and voltage compensation of microgrids using radial basis function neural network-based harmonic power-flow calculations for distributed and decentralised control structures," *IET Gener., Transmiss. Distrib.*, vol. 12, no. 7, pp. 1518–1530, Apr. 2018.

[15] N. Yang, R. Huang, and M. Guo, "Three-phase feeder parameter estimation using radial basis function neural networks and multi-run optimisation method with bad data preparation," *IET Gener., Transmiss. Distrib.*, pp. 1–13, Oct. 2021.

[16] L. N. D. Castro and F. J. V. Zuben, "A pruning self-organizing algorithm to select centers of radial basis function neural networks," in *Artificial Neural Nets and Genetic Algorithms*. Vienna, Austria: Springer, 2001, pp. 114–117.

[17] H. Demuth and M. Beale, "Neural network toolbox," *Mathworks*, vol. 21, no. 15, pp. 1225–1233, 2007.

[18] A. Abur and A. G. Exposito, "Power system state estimation: Theory and implementation," *Universiti Teknologi Petronas*, vol. 17, no. 95, pp. 213–256, 2004.

[19] W. H. Kersting, "Radial distribution test feeders," *IEEE Trans. Power Syst.*, vol. 6, no. 3, pp. 975–985, Aug. 1991.

[20] N. Yang, "Three-phase power flow calculations using direct z BUS method for large-scale unbalanced distribution networks," *IET Gener., Transmiss. Distrib.*, vol. 10, no. 4, pp. 1048–1055, Mar. 2016.

[21] P. Subcommittee, "IEEE reliability test system," *IEEE Trans. Power App. Syst.*, vol. PAS-98, no. 6, pp. 2047–2054, Nov. 1979.

NIEN-CHE YANG (Member, IEEE) was born in Keelung, Taiwan, in 1977. He received the B.S., M.S., and Ph.D. degrees in electrical engineering from the National Taiwan University of Science and Technology, Taipei, Taiwan, in 2002, 2004, and 2010, respectively. Since 2018, he has been with the faculty of the National Taiwan University of Science and Technology, where he is currently an Associate Professor of electrical engineering. His research interests include micro-grid state estimation, harmonic three-phase power flow analysis, probabilistic three-phase power flow analysis, energy loss computation in low voltage networks, micro-grids, smart grids, and electric vehicles. He is a member of the Phi Tau Phi Scholastic Honor Society.

RUI HUANG received the master's degree from Yuan-Ze University, Taoyuan, Taiwan, in 2019. His research interests include parameter estimation and state estimation.

MOU-FA GUO was born in Fujian, China, in 1973. He received the B.S. and M.S. degrees in electrical engineering from Fuzhou University, Fuzhou, China, in 1996 and 1999, respectively. Since April 2000, he has been with Fuzhou University, where he is currently a Professor and the Chairperson of the Department of Electric Power Engineering. He is the author of two books, more than 50 articles, and holds more than ten patents. His research interests include power distribution systems and automation.